

# Dithiocarbonate and trithiocarbonate interactions with pyrite

J.A. Venter<sup>\*†</sup> and M.K.G. Vermaak<sup>\*</sup>

Dithiocarbonate (xanthate) collectors have been the workhorse of the sulphide flotation industry for more than 80 years. More recently, some flotation plants have started to use a new collector, trithiocarbonate (TTC). Extensive research has been conducted on the interaction of different substrates with xanthates, which adsorb electrochemically and are present as a chemisorbed xanthate, metal xanthate or dixanthogen. The work reported here is the first detailed, fundamental evaluation of a long-chain trithiocarbonate collector for sulphide minerals. The results show that this collector—unlike the widely used xanthate collector—has a strong non-electrochemical collection action in addition to an electrochemical one. The non-electrochemical action opens up significant possibilities of changing mill conditions (specifically regarding the propensity of sulphide minerals to oxidize), to obtain better sulphide recovery.

## Introduction

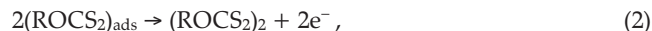
Flotation is a versatile and important concentration step for low-grade and complex ores that need to be ground very finely to achieve liberation. Collectors are added to a mixture of ore particles and water, commonly known as pulp. These collectors are surface active chemicals that selectively adsorb onto the minerals of interest. The target mineral is rendered hydrophobic by the collector. When gas (either air or nitrogen) is passed through the pulp, the gas bubbles attach to the hydrophobic particles and the particle–bubble collectives then rise to the surface of the pulp, where the target mineral is concentrated.

<sup>\*</sup>Department of Materials Science and Metallurgical Engineering, University of Pretoria, Pretoria 0002, South Africa.

<sup>†</sup>Author for correspondence. E-mail: albert.venter@eng.up.ac.za

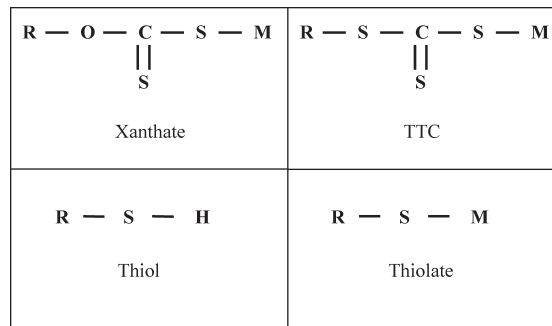
Flotation is used extensively in the base metal, gold and platinum-group element (PGE) industries. In the latter two, although less frequently in the gold industry, the noble elements can be associated with base metal sulphides, e.g. pyrite in the case of gold. Thus, by concentrating these base metal sulphides the noble metals are co-concentrated.

Extensive work has been conducted on the interaction of different thiol collectors with different substrates.<sup>1,2</sup> In the case of dithiocarbonate (xanthate) (see Fig. 1), it has been found that the collector can be present as the monomer or the dimer on the mineral surface and either species can induce flotation.<sup>2</sup> Woods<sup>1</sup> indicated that the adsorption onto gold and pyrite follows similar mechanisms. The formation of dixanthogen occurs through a two-step process:



where R is a hydrocarbon chain.

The first step is the chemisorption of the xanthate onto the surface of the substrate. This is followed by the oxidation of the xanthate to the dixanthogen. According to Woods,<sup>3</sup> the dixanthogen forms multilayers that are physically adsorbed rather than chemisorbed on the surface. This was deduced from the dixanthogen's electrochemical properties. Woods *et al.*<sup>4</sup> showed spectroelectrochemically, with the use of surface-enhanced Raman scattering (SERS) on the surface of a gold



R : non-polar organic hydrocarbon chains

M : alkaline metal

**Fig. 1.** Structures of collector species.

substrate, that a layer of xanthate chemisorbed with multilayers of dixanthogen physically adsorbed onto this layer.

More recently, trithiocarbonates (TTC) (Fig. 1) have also been employed in the recovery of base metal sulphides. Indications are that improved grades and recoveries are realized with the use of TTCs.<sup>5-7</sup> However, the best flotation results were obtained by replacing a small amount of xanthate (less than 25 molar percentage) with an equal-molar quantity of TTC.<sup>5</sup> Initial work by Du Plessis *et al.*<sup>6,7</sup> indicated that it is possible to achieve sufficient hydrophobicity at potentials significantly lower than the standard redox potential [-100 mV (SHE)] of the TTC monomer/dimer couple. This indicates that, in the case of TTC, possibly only the monomer is present or—as stated by Du Plessis *et al.*<sup>6,7</sup>—a decomposition product of the TTC.

The work reported here investigated the mechanism of adsorption of the TTC onto the surface of pyrite, which is compared with the adsorption of xanthate on pyrite. This was performed by the use of contact angle measurements, electrochemistry and Raman spectroscopy.

The first aim with Raman spectroscopy was to establish whether it was possible to detect the interaction of xanthate with pyrite *in situ*. Previous Raman spectroscopy work<sup>4</sup> used gold as a substrate, where SERS is possible; this is not the case with pyrite. Second, having established that Raman spectroscopy can detect xanthate interaction with pyrite, it was used to determine whether the TTC collection mechanism on pyrite was the same as that of xanthate. The contact angle measurements and electrochemistry complemented the Raman spectroscopy.

## Experimental

**Collectors.** Potassium ethyl xanthate (KEX) was purified by recrystallization from acetone by the addition of diethyl ether. The purified xanthate was stored under vacuum in a desiccator. Potassium dodecanetrithiocarbonate ( $C_{12}$ -TTC) was synthesized by the addition of disulphide to the solution of potassium hydroxide in dodecanethiol.<sup>8</sup> The  $C_{12}$ -TTC was stored under vacuum in a desiccator.

**Electrodes.** A natural crystal of pyrite from Ward's Natural Science Establishment that came from Zacatecas, Mexico, was used as an electrode. The pyrite was embedded in a resin and a geometric surface of approximately 0.1 cm<sup>2</sup> was exposed.

**Electrochemical measurements.** The electrochemical cell and set-up are described elsewhere.<sup>9</sup> The same general procedure was followed. Potentials were measured against a Ag/AgCl reference electrode filled with saturated KCl, which has a potential of +0.20 V against a standard hydrogen electrode (SHE). Experiments were conducted at 25 ± 1°C and in a 0.05 M sodium borate buffer ( $Na_2B_4O_7$ ) solution (pH 9.3). The following was also done:

- The pyrite surface was wet ground using 2400 grit silicon carbide paper.
- The surface was then polished with a suspension of 0.05 μm Micropolish Alumina-B.
- Scans were performed in fresh de-aerated solutions.
- Cyclic voltammograms were recorded after the open-circuit potential had stabilized.
- Cyclic voltammograms were recorded by changing the potential linearly with time from the most negative potential to the upper potential and back at a rate of 1 mV/s.

**Contact angle measurements.** The same experimental set-up and procedures, as previously described,<sup>9</sup> were used for the determination of the contact angles. The contact-angle cell was washed with chromic acid between every experimental run, to avoid contamination by the different collectors. As was the case with

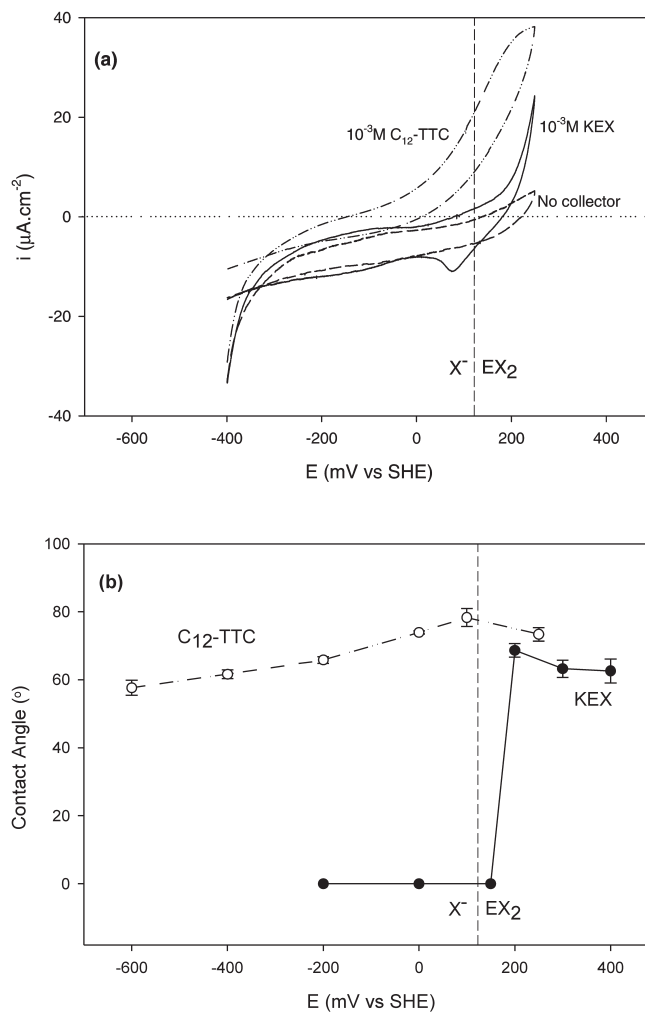


**Fig. 2. a,** Cyclic voltammograms, scanned at 1 mV/s, of pyrite in 0.05 M borate solutions with no collector, 10<sup>-3</sup> M KEX and 10<sup>-3</sup> M C<sub>12</sub>-TTC; **b,** contact angles for pyrite electrode polarized for 300 s in 0.05 M borate solutions with 10<sup>-3</sup> M KEX and 10<sup>-3</sup> M C<sub>12</sub>-TTC.

the electrochemical experiments, the surface of the pyrite was freshly prepared between experimental runs. Repeatable contact angles were obtained by ensuring a completely flat electrode surface. The electrode was polarized potentiostatically for 300 s before a nitrogen bubble was employed during the contact angle measurements.

**Raman spectroscopy.** *In situ* measurements on the pyrite electrode were made to investigate the interaction of the collectors with the pyrite surface at applied potentials. The set-up and procedures used for the Raman experiments are described elsewhere.<sup>9</sup> A fresh pyrite surface was prepared between experimental runs by silicon carbide grinding followed by wet polishing with alumina-B slurries.

## Results and discussion

### Electrochemical measurements

Figure 2(a) shows cyclic voltammograms that were recorded by changing the potential linearly with time between -400 mV (SHE) and 250 mV (SHE) at a scan rate of 1 mV/s. At the lower potentials, in all three cases, a cathodic current was visible. This cathodic current was probably due to the presence of iron oxide and thus was caused by the change in valence state of the iron.<sup>10</sup> The presence of the hydrophilic iron oxides was likely to be responsible for the small difference between the potential where

dixanthogen can form and that where a finite contact angle was measured [see Fig. 2(b)].

The cyclic voltammogram of the pyrite in the 0.05 M borate solution (without collectors) had a small cathodic current up to approximately 150 mV (SHE), probably due to the presence of iron oxides. There was no significant oxidation detected in the region of -400 mV (SHE) to 250 mV (SHE), resulting in the absence of a cathodic peak on the return cathodic scan. This compares well with previous work.<sup>11</sup>

In the presence of  $10^{-3}$  M KEX, there was a strong anodic peak visible from potentials higher than the reversible potential of the xanthate/dixanthogen couple [121 mV (SHE)].<sup>9</sup> On the return cathodic sweep, a cathodic peak was visible from approximately +120 mV; this cathodic peak was due to the reduction of the dixanthogen formed during the anodic scan.<sup>10</sup>

Bubble contact was possible only when the pyrite electrode was polarized at potentials more positive than the reversible potential of the xanthate/dixanthogen couple. These results are in good agreement with previous work.<sup>10</sup>

The results for  $C_{12}$ -TTC were significantly different from those of the xanthate. It was possible to measure finite contact angles even when only cathodic currents were detected. However, there was an increase of approximately  $10^\circ$  in the contact angle at a potential greater than -200 mV (SHE). From the cyclic voltammogram [see Fig. 1(a)], it is possible to see that a significant anodic current is present from above -150 mV (SHE). There is, however, no cathodic peak present on the return cathodic scan. This indicates that the reaction responsible for the anodic current is not reversible. Cyclic voltammograms of TTC on a gold substrate reported by Groot *et al.*,<sup>12</sup> also indicated the absence of a reduction peak.

Some kind of product layer was visually detected at very low potentials (-200 mV). This correlates with findings from Groot *et al.*,<sup>12</sup> which are briefly summarized as follows. Surface plasmon resonance (SPR) allows for the determination of the presence of material on the surface of the gold substrate. In the case of the xanthate collector, there is only a change in the SPR angle (amount of collector on the surface) at potentials higher than the reversible potential of the xanthate/dixanthogen couple. Below this potential no collector is detected; this corresponds to insignificant changes in the SPR angle. In the case of the TTC, there is a significant change in the SPR angle from potentials where anodic currents are measured, but, importantly, below this potential a small SPR angle was also measured. This indicates that there was some material present at low potentials before any electrochemical reaction was measured. In addition, it indicates an increase in the amount of material present on the gold surface at potentials where anodic currents are detected. This correlates well with the findings in this study (see Fig. 2), showing an increase in the contact angle at potentials where anodic currents are measured.

The maximum contact angles measured in the xanthate solution were as expected (approximately  $70^\circ$ ); however, in the case of  $C_{12}$ -TTC, greater angles than those measured (approximately  $75^\circ$ ) would be expected due to its longer chain length.<sup>10</sup> The reason for the contact angles being smaller than expected is the stabilization of the bubble by the  $C_{12}$ -TTC as illustrated by bubble behaviour in contact with the pyrite surface. In Fig. 3(a) the contact angle obtained only by collision of the bubble with the surface is approximately  $70^\circ$ ; the figure shows also the same bubble after the electrode was carefully vibrated — the contact angle changed to approximately  $90^\circ$ . This is closer to the expected values for long-chain collectors. In the case of the xanthate collector there was no significant change in the contact angle

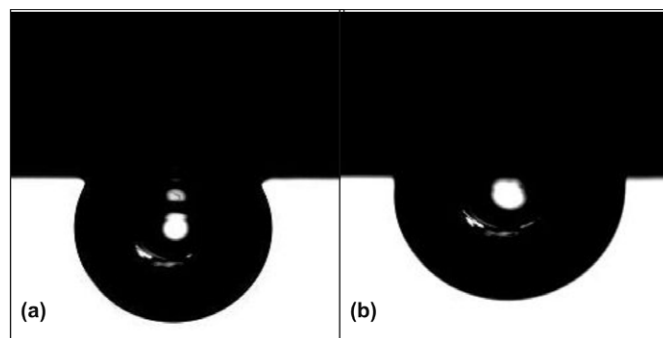


Fig. 3. a, Bubble due to collision with the surface of a pyrite electrode in a 0.05 M borate and a  $10^{-3}$  M  $C_{12}$ -TTC solution polarized for 300 s; b, same bubble after electrode was vibrated.

when the pyrite electrode was vibrated. Visual observations during the experimental runs indicated longer induction times for the bubbles in the  $C_{12}$ -TTC solutions compared to those in the xanthate solutions. Breytenbach *et al.*<sup>5</sup> alluded to the stabilizing effect of TTC, reporting the formation of more stable froths during batch flotation experiments, resulting in higher mass pulls. A further indication of the influence of  $C_{12}$ -TTC on the bubble stability was evident when the concentration of the collector was decreased during contact angle measurements. It was possible to achieve contact angles of approximately  $100^\circ$  (collision only) in  $10^{-5}$  M  $C_{12}$ -TTC solutions compared to the approximately  $70^\circ$  achieved in the  $10^{-3}$  M solution; with the lower bulk concentration of the TTC, one would expect that the interfacial concentration of the TTC should be lower and thus reduce the stabilization effect of the TTC.

The electrochemical and contact angle measurements show that  $C_{12}$ -TTC rendered the pyrite surface hydrophobic at significantly more negative potentials than the xanthate collector. The contact angle measurements also indicated that the  $C_{12}$ -TTC significantly stabilized the bubbles. The latter effect is counter-productive, since one of the ideal characteristics of a collector is that it should have weak frothing characteristics.<sup>13</sup>

#### Raman spectroscopy

The Raman spectrum of pyrite was recorded in borate solution (without collectors). Two very intense peaks were visible between  $300\text{ cm}^{-1}$  and  $400\text{ cm}^{-1}$ . These peaks were due to the Fe-S bonds that are present in pyrite.<sup>14</sup> Raman spectra for the experimental work on pyrite were recorded from above  $400\text{ cm}^{-1}$  to preclude these intense peaks from interfering with the interpretation of the spectra of the adsorbed species. In most of the Raman spectra a band at approximately  $870\text{ cm}^{-1}$  was visible. This band was a result of the borate buffer solution.<sup>15</sup>

Figure 4 shows the Raman spectra of purified KEX and freshly synthesized diethyl dixanthogen ( $EX_2$ ) as reference. The characteristic Raman bands are listed in Table 1. Figure 4 also shows the *in situ* Raman spectra of a pyrite electrode polarized at 250 mV (SHE) for different lengths of time in 0.05 M borate and  $10^{-3}$  M KEX solutions. From the *in situ* spectra significant Raman bands appeared only after 240 s. The only species that can be identified is the dixanthogen by the appearance of two intense peaks at  $428\text{ cm}^{-1}$  (C-O-C *trans* deformation) and  $498\text{ cm}^{-1}$  (S-S stretching vibration). The S-S stretch band especially is significant because this peak is not present in the case of the xanthate monomer. There were no peaks in the *in situ* Raman spectrum that indicate the presence of the xanthate monomer.

From the Tafel slopes of the anodic peak measured during cyclic voltammetry of pyrite, we concluded that the oxidation of

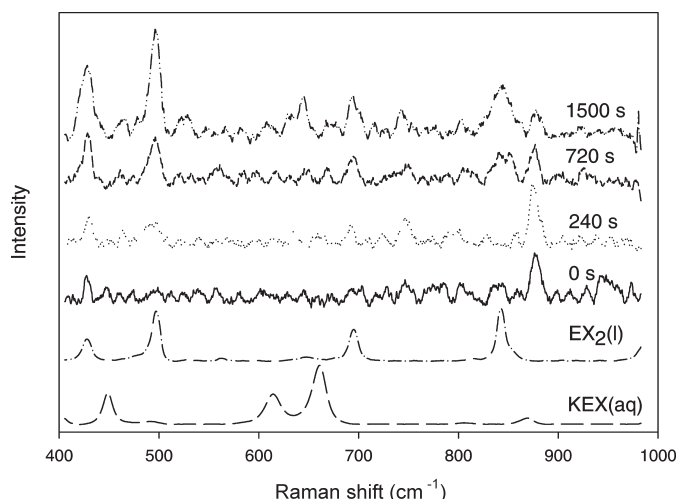


**Fig. 4.** Comparison of the spectra of xanthate and dioxanthogen against the spectra of a pyrite electrode polarized at 250 mV (SHE) for different times in a 0.05 M borate and a  $10^{-3}$  M KEX solution.

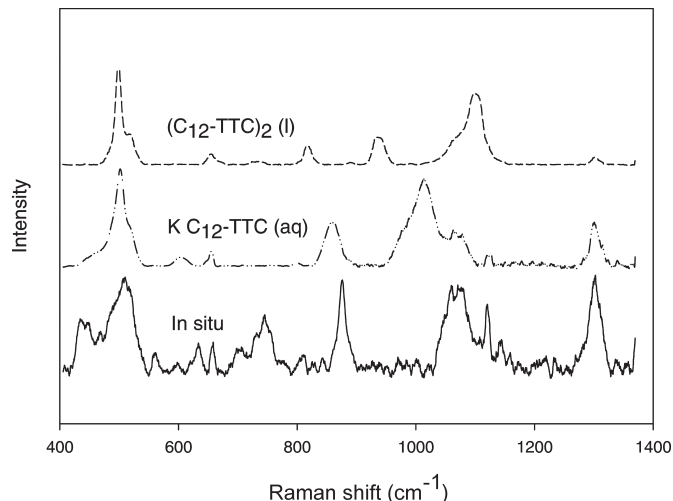
the xanthate was preceded by the chemisorption of the xanthate monomer.<sup>1</sup> It is reported that the mechanism of the interaction of xanthate with pyrite is similar to that of gold. The chemisorption of the monomer on gold was spectrochemically verified by Woods *et al.*<sup>4</sup> The phenomenon of surface-enhanced Raman scattering occurs on gold, which makes it possible to achieve  $10^3$  times higher sensitivity when recording Raman spectra. Woods *et al.*<sup>4</sup> deduced from their measurements that there was a layer of chemisorbed xanthate on the surface with multilayers of dioxanthogen bonded to this layer. This was deduced from the fact that the band intensities of the chemisorbed xanthate and dioxanthogen were similar even though the concentration of the dioxanthogen was much higher. In the case of pyrite no surface enhancement is possible. It was hence possible to detect the dioxanthogen only after 240 s of polarization when the concentration was high enough through the formation of multilayers of dioxanthogen. There was no measurable evidence of any chemisorbed xanthate, presumably because the concentration of the chemisorbed xanthate was very low, possibly only a monolayer.

Figure 5 shows the Raman spectra of potassium dodecanethiocarbonate ( $KC_{12}$ -TTC) and didodecane dithiocarbonate ( $C_{12}$ -TTC<sub>2</sub>) compared to the Raman spectrum of the pyrite electrode in 0.05 M borate and  $10^{-3}$  M  $KC_{12}$ -TTC solutions, after polarization at 0 mV (SHE) for 900 s. It is clear from these spectra that the species detected on the surface was neither of the two TTC species. The peak at approximately  $740\text{ cm}^{-1}$  is characteristic

**Table 1.** The comparative Raman bands of potassium ethyl xanthate and of diethyl dioxanthogen.

Vibration	Raman shift ( $\text{cm}^{-1}$ )			
	Woods <i>et al.</i> <sup>4</sup>		Vermaak <i>et al.</i> <sup>9</sup>	
	KEX (aq)	EX <sub>2</sub> (l)	KEX (aq)	EX <sub>2</sub> (l)
CS <sub>2</sub> antisymmetric stretch	1046	1041	1046	1041
CCOC stretch	864	845	864	844
CS <sub>2</sub> symmetric stretch <i>trans</i>	660	695	659	694
CS <sub>2</sub> symmetric stretch <i>gauche</i>	615	646	614	646
OCS <sub>2</sub> out of plane <i>wag</i>	556	528	—	—
SS stretch	n.a.	498	n.a.	498
COC deformation <i>gauche</i>	493	473	493	—
COC deformation <i>trans</i>	449	427	448	428
OCC deformation	399	378	401	378

n.a., not applicable; l, liquid; aq, aqueous solution.

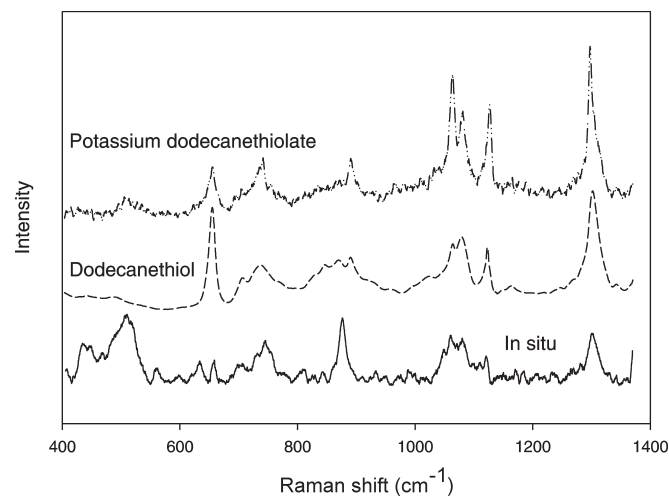


**Fig. 5.** Raman spectra of  $C_{12}$ -TTC monomer and dimer compared to the *in situ* spectrum of a pyrite electrode in a 0.05 M borate and a  $10^{-3}$  M potassium dodecanethiocarbonate solution polarized at 0 mV (SHE) for 900 s.

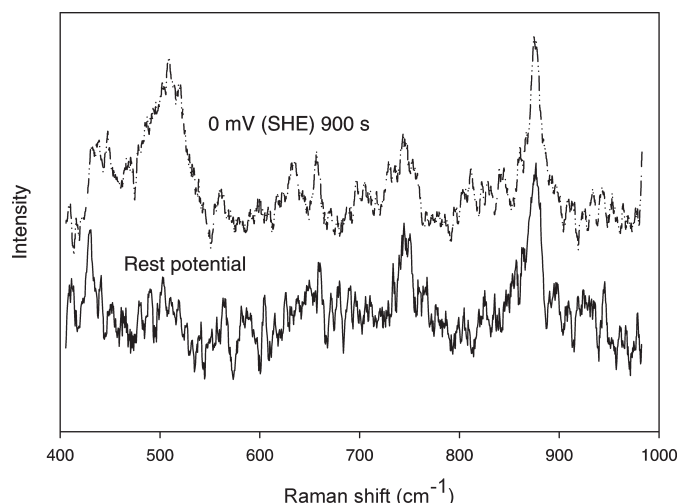
of the  $\nu(\text{C-S})$  band for adsorbed alkanethiols.<sup>16</sup>

Figure 6 shows the Raman spectra of the dodecanethiol and potassium dodecanethiolate (Fig. 1) compared to the Raman spectrum of the pyrite electrode in 0.05 M borate and  $10^{-3}$  M  $KC_{12}$ -TTC solutions polarized at 0 mV (SHE) for 900 s. From these spectra it is evident that there is a strong similarity between the three species. Table 2 summarizes data from the literature on some of the most important Raman bands found in the region of interest. These peaks (see Table 2) had been determined with SERS; the peak intensity and resolution were much higher than in the present case. It is interesting to note that the peak at approximately  $740\text{ cm}^{-1}$  is attributed to the *trans* conformer of the S-C-C chain. This peak is visible in all three spectra, while the peak at approximately  $655\text{ cm}^{-1}$  (the *gauche* conformer of the S-C-C chain) is visible only in the thiol and thiolate spectra. This indicates that the *in situ* species is probably the *trans* conformer.

There is some additional activity in the region of  $400\text{--}550\text{ cm}^{-1}$ , with the *in situ* spectrum, that is not present in the case of the thiol species. In Fig. 7 it is possible to see that there are some thiol species present at the rest potential even though no anodic current is present. Compared to the spectra of the pyrite surface polarized at 0 mV (SHE) for 900 s, the main difference is the presence of the wide band in the region of  $400\text{--}550\text{ cm}^{-1}$ . This



**Fig. 6.** Raman spectra of the  $C_{12}$ -thiol and  $C_{12}$ -thiolate compared to the *in situ* spectrum of a pyrite electrode in a 0.05 M borate and a  $10^{-3}$  M potassium dodecanethiocarbonate solution polarized at 0 mV (SHE) for 900 s.



**Fig. 7.** Raman spectra and the *in situ* spectra of a pyrite electrode, in a 0.05 M borate and a  $10^{-3}$  M potassium dodecanethiocardonate solution polarized, at 0 mV (SHE) for 900 s and at its rest potential.

**Table 2.** Characteristic Raman bands of thiols adsorbed on metals.<sup>16</sup>

Vibration	Raman shift ( $\text{cm}^{-1}$ )
$\text{CH}_2$ wagging	~1300
$\nu(\text{C}-\text{C})$	1000–1100
$\text{CH}_3$ rocking	900
$\text{CH}_2$ rocking	700–900
$\nu(\text{C}-\text{S})_{\text{T}}$	700–740
$\nu(\text{C}-\text{S})_{\text{G}}$	620–650

indicates that the TTC species, which also shows bands in this region (Fig. 5), may be present at more positive potentials. Thus, the TTC may serve as an absorption intermediate for the attachment of the thiol species.

## Conclusions

In the interaction of xanthate with pyrite, the presence of the xanthate could be detected only above the reversible potential of the xanthate/dixanthogen couple [121 mV (SHE)]. Dixanthogen was the only species that could be determined spectrochemically, although both it and the chemisorbed xanthate should have been present.

In the interaction of TTC with pyrite, a hydrophobic surface could be created at potentials below  $-200$  mV (SHE), when only a cathodic current was present. At potentials higher than  $-200$  mV (SHE), the contact angles increased by approximately  $10^\circ$ . Raman spectroscopy indicated that thiol species were present on the surface rather than the TTC itself; this is in agreement with the findings of Du Plessis *et al.*<sup>6,7</sup> It also indicated that the TTC possibly serves as an intermediate step for the adsorption of

the collector onto the surface of the pyrite. This would account for the increase of the contact angle above  $-200$  mV (SHE), because the TTC interacts electrochemically with the surface above this potential. We conclude that as soon as the TTC is adsorbed, it decomposes to the thiol species.

Electrochemical and Raman spectroscopy would have to be conducted on the interaction of the thiol species with pyrite, to verify that the TTC serves as an adsorption intermediate. Moreover, the stability of the TTC, needs to be determined, to indicate whether the thiol species detected on the surface of the pyrite, in reducing conditions, is due to the decomposition of the TTC in solution.

Received 1 June. Accepted 30 September 2006.

- Woods R. (1996). Chemisorption of thiols on metals and metal sulfides. *Mod. Aspects Electrochem.* **29**, 401–453.
- Finkelstein N.P. and Poling G.W. (1977). The role of dithiolates in the flotation of sulphide minerals. *Mineral Sci. Engng* **9**(4), 177–197.
- Woods R. (1971). The oxidation of ethyl xanthate on platinum, gold, copper and galena electrodes. Relation to the mechanism of mineral flotation. *J. Phys. Chem.* **75**(3), 354–362.
- Woods R., Hope G.A. and Brown G.M. (1998). Spectroelectrochemical investigations of the interaction of ethyl xanthate with copper, silver and gold: III. SERS of xanthate adsorbed on gold surfaces. *Colloids and Surfaces A: Physicochem. Engng Aspects* **137**, 339–344.
- Breytenbach W., M.K.G. Vermaak and Davidtz J.C. (2003). Synergistic effects among dithiocarbonates (DTC), dithiophosphate (DTP) and trithiocarbonates (TTC) in the flotation of Merensky ores. *J. S. Afr. Inst. Min. Metal.* **103**, 667–670.
- Du Plessis R., Miller J.D. and Davidtz J.C. (2000). Preliminary examination of electrochemical and spectroscopic features of trithiocarbonate collectors for sulfide mineral flotation. *Trans. Nonferrous Met. Soc. China* **10**, 12–18.
- Du Plessis R., Miller J.D. and Davidtz J.C. (2002). The development of trithiocarbonate collectors for precious metals recovery by sulphide mineral flotation. In *Proc. 26th International Precious Metals Conference*, Miami.
- Drake J.E. and Yang J. (1994). Synthesis and spectroscopic characterization of *S*-ethyl, *S*-isopropyl, *S*-*n*-propyl and *S*-*n*-butyl trithiocarbonate (trixanthate) derivatives of trimethyl- and triphenylgermane and diphenyldigermane. Crystal structure of  $\text{Ph}_2\text{Ge}[\text{S}_2\text{CS}(i\text{-Pr})_2]_2$ . *Inorg. Chem.* **33**, 854–860.
- Vermaak M.K.G., Pistorius P.C. and Venter J.A. (2005). Electrochemical and Raman spectroscopic studies of the interaction of ethyl xanthate with Pd-Bi-Te. *Minerals Engng* **18**, 575–584.
- Gardner J.R. and Woods R. (1977). An electrochemical investigation of contact angle and of flotation in the presence of alkylxanthates. II Galena and pyrite surfaces. *Aust. J. Chem.* **27**, 981–991.
- Woods R. (1976). Electrochemistry of sulphide flotation. In *Flotation: A.M. Gaudin Memorial Volume*, vol. 1, ed. M.C. Feurstenau, pp. 298–333. Port City Press Inc., Baltimore.
- Groot D.R., Harkema S.H.M. and Vermaak M.K.G. (2005). The application of cyclic voltammetry coupled with surface plasmon resonance measurements to thiol-collector interactions with gold surfaces. *J. S. Afr. Inst. Min. Metal.* **105**, 645–652.
- Wills B.A. (1997). In *Mineral Processing Technology*, 6th edn., chap. 12, pp. 258–341. Butterworth Heinemann, Oxford.
- McGuire, M.M., Jallad, K.N., Ben-Amotz, D. and Hamers, R.J. (2001). Chemical mapping of elemental sulfur on pyrite and arsenopyrite surfaces using near-infrared Raman imaging microscopy. *Appl. Surf. Sci.* **178**, 105–115.
- Oblonsky L.J. and Devine T.M. (1995). A surface enhanced Raman spectroscopic study of the passive films formed in borate buffer on iron, nickel, chromium and stainless steel. *Corrosion Sci.* **37**, 17–41.
- Kudelski A. (2005). Characterization of thiolate-based mono- and bilayers by vibrational spectroscopy: a review. *Vibrational Spectroscopy* **39**, 200–213.